

# Raman Assessment of Bone Quality

Michael D. Morris PhD, Gurjit S. Mandair PhD

Published online: 30 November 2010  
© The Association of Bone and Joint Surgeons® 2010

## Abstract

**Background** Progress in the diagnosis and prediction of fragility fractures depends on improvements to the understating of the compositional contributors of bone quality to mechanical competence. Raman spectroscopy has been used to evaluate alterations to bone composition associated with aging, disease, or injury.

**Questions/purposes** In this survey we will (1) review the use of Raman-based compositional measures of bone quality, including mineral-to-matrix ratio, carbonate-to-phosphate ratio, collagen quality, and crystallinity; (2) review literature correlating Raman spectra with biomechanical and other physiochemical measurements and with bone health; and (3) discuss prospects for ex vivo and in vivo human subject measurements.

**Methods** ISI Web of Science was searched for references to bone Raman spectroscopy in peer-reviewed journals. Papers from other topics have been excluded from this review, including those on pharmaceutical topics, dental tissue, tissue engineering, stem cells, and implant integration.

**Results** Raman spectra have been reported for human and animal bone as a function of age, biomechanical status, pathology, and other quality parameters. Current literature

supports the use of mineral-to-matrix ratio, carbonate-to-phosphate ratio, and mineral crystallinity as measures of bone quality. Discrepancies between reports arise from the use of band intensity ratios rather than true composition ratios, primarily as a result of differing collagen band selections.

**Conclusions** Raman spectroscopy shows promise for evaluating the compositional contributors of bone quality in ex vivo specimens, although further validation is still needed. Methodology for noninvasive in vivo assessments is still under development.

## Introduction

Raman spectroscopy is a vibrational spectroscopy technique used to assess scattered light from biologic molecules and ions. Raman scattering occurs when molecules within a specimen are excited by incident laser light. Vibrational motions within the molecules lead to a small fraction of the light (approximately one in  $10^7$  photons) losing energy and being scattered at longer wavelengths [7]. The wavelength difference between scattered and incident light corresponds to molecular vibrations and leads to bands at characteristic frequency shifts in the Raman spectrum. These shifts are labeled in wavenumber units corresponding to the vibrational energy ( $\text{cm}^{-1}$ ). Frequency shifts serve as an important source of contrast in assessing tissue composition such as carbonate substitutions for phosphate positions in bone. The extracellular matrix also provides another source of contrast to bone tissue composition. The extracellular matrix contains many protein-rich vibrational modes, corresponding predominantly to collagen features such as amide backbone, protein secondary structure, and side chain composition.

---

One or more of the authors (MDM) has an equity interest in BioMatrix Photonics, LLC. One or more of the authors (MDM) received funding from grants from the National Institutes of Health grants R01 AR055022 and R01 AR054496.

---

M. D. Morris, G. S. Mandair  
University of Michigan, Ann Arbor, MI, USA

M. D. Morris (✉)  
Department of Chemistry, University of Michigan, 930 N  
University Avenue, Ann Arbor, MI 48109-1055, USA  
e-mail: mdmorris@umich.edu

Raman and Fourier transform infrared (FTIR) spectroscopies provide almost equivalent chemical information on bone tissue composition, because both methods measure partially overlapping subsets of the vibrational spectrum [14, 23]. The main advantages of Raman spectroscopy include its applicability to fresh tissue [24, 74] and higher spatial resolution (with sampling volumes of  $1 \mu\text{m}^3$  or less) [25]. Raman spectroscopy can also be used with fixed and embedded specimens [32, 80] and also to fluorescently labeled and stained specimens [21, 52, 75], although heavy staining may facilitate burning [50]. When combined with mechanical loading regimes, Raman spectroscopy correlates chemical information with bone failure responses at the ultrastructural level [15]. Fiberoptic probes that allow noninvasive *in vivo* Raman spectroscopy are now under development [45, 66].

There are, however, several important limitations to Raman spectroscopy. At this writing, only the major components of bone have been observed spectroscopically, namely mineral phosphate, carbonate, and matrix collagen. Bone lipids and phospholipids have also been observed [41, 57], although they maybe inaccessible as a result of removal during specimen preparation.

Noncollagenous proteins (NCPs) almost certainly contribute to the bone Raman spectrum [19], but their low abundance and spectral similarity with collagen [19, 57] make them difficult to isolate spectroscopically in whole bone specimens. In contrast, fluorescent blood products in bone cause intense background features, which can obscure bone Raman spectra [68]. Tissue fluorescence can be minimized by using longer wavelength excitation light (785-nm lasers in near-infrared are commonly used) or using photobleaching protocols for shorter wavelength excitation sources (such as 532 nm lasers) [50, 75]. Fresh, intact, hydrated bone specimens are widely preferred in Raman spectroscopy. Embedding media such as polymethylmethacrylate (PMMA) may increase the variance in measurements extracted from bone Raman spectra [80]. Minor contributions from embedding media can be removed by subtracting appropriately scaled reference spectra (such as pure PMMA) [4]. For extensive spectral interference, alternative embedding media [80], more advanced spectral subtraction methods [74], or even greater numbers of specimens can be sought to detect differences between different experimental groups. Because of the small portion of scattered light, Raman acquisition times can be one to two orders of magnitude higher than those typically used in infrared spectroscopy [40, 62]. This significant limitation in acquiring large Raman images of bone might be particularly important if heterogeneity of bone tissue composition is eventually proven to be a major contributor to fracture resistance (ie, to bone quality). At present, multiple Raman spectra are collected to construct

histograms required for heterogeneity measurements [82], whereas pixel histograms have routinely been extracted from bone FTIR images [29].

The term “bone quality” refers to the ensemble of composition and architectural properties of bone tissue that together determine its material properties and its ability to perform its mechanical functions [34]. Raman spectroscopy yields at least four important composition measures that are components of bone quality. These are: mineral-to-matrix ratio, carbonate-to-phosphate ratio, mineral crystallinity, and the collagen quality parameter. We define and review each of these components to bone quality in turn and highlight some of their limitations. We emphasize papers published within the last decade. We review how Raman spectroscopy is used to study age-related changes in bone, osteoporosis, and various genetic disorders. The effects of orientation, fractures, chemical, and radiologic insults to bone composition are reviewed. Finally, we describe the use of noninvasive Raman spectroscopy, which may allow the clinician to assess bone quality *in vivo*.

## Materials and Methods

We used the ISI Web of Knowledge database to identify initially 645 articles containing the terms “Raman” AND “bone.” To narrow the number of articles identified, we used additional terms: “age,” “osteoporosis,” “fracture,” and “mineral,” which resulted in 52, 39, 60, and 159 hits, respectively. The searches focused primarily on papers published in bone-related journals and bone studies published in peer-reviewed chemical spectroscopy and biomedical optics journals. The searches also included cited crossreferences of the published papers published up to January 2010 with selected papers published up to August 2010. Papers related to dental tissue, stem cells, tissue engineering, and pharmaceutical topics were excluded. The selected papers were reviewed individually to yield 56 papers for this review.

## Contribution of Collagen and Mineral to Bone Quality

Work in this field owes much to earlier FTIR studies of bone [12, 49, 54]. Armed with this knowledge, early workers in bone Raman spectroscopy used or modified infrared correlations to interpret Raman bone spectra. As shown (Fig. 1), most of the bands of a bone Raman spectrum can be assigned to mineral phosphate, carbonate, or matrix collagen. However, absolute band intensities are seldom used in Raman spectroscopy because they are affected by Raman scattering efficiency and other optical

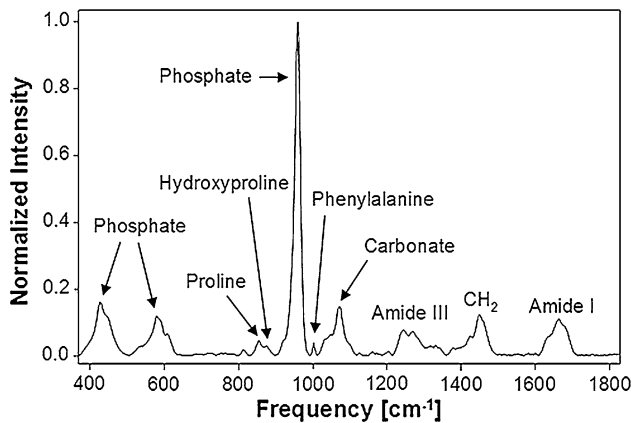


**Fig. 1** Raman spectrum taken from the tibia of 6-week-old mouse bone showing the assignments for bone mineral and matrix-specific Raman bands. The spectrum was acquired using 785 nm excitation, baseline-corrected, and then normalized to the intensity of the symmetric phosphate band near  $959\text{ cm}^{-1}$ .

effects such as grain size, refractive index, and surface roughness of the specimen [79]. For these reasons, many studies report the relative peak intensities or peak areas (ie, integrated peak intensities) of select pairs of bands from the Raman spectrum. For instance, dividing the primary phosphate band (approximately  $959\text{ cm}^{-1}$ ) by the amide I band ( $1616\text{--}1720\text{ cm}^{-1}$ ) corresponds to the mineral-to-matrix ratio, which indicates the amount of mineralization [48]. Raman mineral-to-matrix ratios have not been calibrated with measured materials such as the ash weight of bone. Nevertheless, these ratios can be used to assess compositional trends in a series of related specimens such as the increased age-related mineralization trends observed in mouse calvarial tissues [73] and rat cortical bone [21]. Matrix bands based on methylene side chains ( $\text{CH}_2$  at  $1450\text{ cm}^{-1}$ ) [69, 80, 82], amide III ( $1243\text{--}1320\text{ cm}^{-1}$ ) [37], phenylalanine (approximately  $1002\text{ cm}^{-1}$ ) [30, 67, 79], CH stretch (approximately  $2940\text{ cm}^{-1}$ ) [69, 70, 79], or the combined proline ( $921$  and  $855\text{ cm}^{-1}$ ) and hydroxyproline ( $876\text{ cm}^{-1}$ ) have also been used [39]. The choice of matrix band is dependent on the embedding conditions, instrumentation, and its orientational sensitivity (or lack of) toward mineralized collagen fibrils. For brevity, only the latter is discussed in this review.

The presence of a prominent carbonate band around  $1070\text{ cm}^{-1}$  in the Raman spectrum (Fig. 1) is significant because it shows phosphate positions in the apatitic lattice are susceptible to ionic substitution. Raman measures of carbonate-to-phosphate (at  $959\text{ cm}^{-1}$ ) ratios can provide valuable insights into the chemical composition of murine or human bones because it varies with bone architecture, age, and mineral crystallinity [3, 43, 82]. However, the carbonate band is partially overlapped by another phosphate band around  $1076\text{ cm}^{-1}$  [5], which can reduce

measurement precision, especially for apatites with minimal carbonate content. Nevertheless, the measurement has been calibrated against carbonated apatitic standards (carbonate-to-phosphate area ratios versus percent carbonate weight) and used to determine the carbonate content of ground bovine bone (approximately  $7.7\% \pm 0.4\%$ ). Another carbonate-related parameter includes carbonate-to-amide I (at  $1665\text{ cm}^{-1}$ ) ratios, which may indicate bone remodeling [48].

The strength of bone is not only dependent on the amount of mineralization, but also on the degree of mineral crystallinity and the optimal distribution of different crystal sizes [11, 53]. The most experimentally accessible Raman measure of mineral crystallinity is the width of the primary phosphate band near  $959\text{ cm}^{-1}$  [3, 5, 18, 24, 28, 58]. A single Gaussian curve is usually used to fit the phosphate band to obtain the full-width half-maximal (FWHM). The fitted band FWHM value is reported as wavenumbers (in  $\text{cm}^{-1}$ ) or as inverse FWHM (units not typically reported). In synthetic carbonated apatites, increased mineral crystallinity yields narrower phosphate bandwidths, which is mirrored by reduced carbonate substitution (ie, reduced carbonate-to-phosphate ratios). For example, hydroxyapatite standards with negligible wt% carbonate yield bandwidths of approximately  $6.7\text{ cm}^{-1}$  compared with  $9.6$  to  $13.6\text{ cm}^{-1}$  for apatites with  $3.5\text{ wt}\%$  carbonate (as determined by coulometric and FTIR analyses) [5]. However, this trend is not always observed in bone specimens [82], because mineral crystallinity can remain unchanged despite the observed increase in carbonate-to-phosphate ratios. Although the *c*-axis length of a subset of apatitic samples (eg, human bone, boar tusk, buffalo enamel, and hydroxyapatite) has been positively correlated with crystallinity ( $R = 99.2\%$ ,  $p < 0.01$ ), the precision of mineral crystallinity measurements is poor because the range of bandwidths possible for a given tissue type is small (approximately  $1\text{--}3\text{ cm}^{-1}$ ) [24, 56].

The collagen quality parameter used in Raman spectroscopy is derived from a subset of partially resolved amide I bands, whose relative intensities depend on its secondary structure. Although theory supports the use of similar bands originally developed by bone infrared spectroscopists to assess nonreducible to reducible collagen crosslink ratios (approximately  $1660/1690\text{ cm}^{-1}$  ratios) [55], there are differences in the spectra and instrumentation that needs to be taken into consideration. First, FTIR microspectrometers yield spectra with superior signal-to-noise (S/N) ratios of approximately 1000:1 compared with approximately 30–80:1 obtained by Raman spectrometers [40, 63]. The low Raman S/N ratio is attributed to the weak scattering that occurs at 785 nm, less than one-fifth of the intensity at 532 nm [27]. Second, the quantum efficiency of the best available CCD detector in the 800 to 900-nm range

(required for 785-nm laser excitation) is approximately 30% to 40% [20, 27]. As a consequence, individual Raman measurements can be made of bone matrix collagen bands in the amide I region (approximately 1620–1710  $\text{cm}^{-1}$ ) have lower S/N ratios and are less precise than single infrared measurements [30, 55]. Raman measurements can be made very precise by averaging multiple Raman spectra from a single Raman image, resulting in S/N ratios of up to 850:1 [40]. Third, bone matrix amide I spectra is sensitive to the excitation wavelength used. For instance, human cortical bone excited at 244 nm (deep ultraviolet) yields a prominent amide I band at approximately 1655  $\text{cm}^{-1}$ , but the underlying 1690  $\text{cm}^{-1}$  peak, which is used as a measure of reducible crosslinks in FTIR, is not detected [55]. Finally, both descriptive and ratiometric terms have been used to assess the collagen quality parameter. In bone deformation studies, a shift in the bone matrix amide I band position from 1665  $\text{cm}^{-1}$  to 1678  $\text{cm}^{-1}$  is indicative of ruptured collagen crosslinks [15], whereas area ratios between 1690  $\text{cm}^{-1}$  and 1660  $\text{cm}^{-1}$  bands are measures of collagen quality of wild-type and biglycan-deficient mice [77, 78]. In a series of deep ultraviolet bone Raman studies, an increase (relative to the  $\text{CH}_2$  band at 1240  $\text{cm}^{-1}$ ) of the amide I band at 1655  $\text{cm}^{-1}$  indicates altered collagen quality induced by aging [2], hydration/dehydration [1], or radiologic damage [6].

Raman compositional measures are correlated with cortical bone stiffness, bending modulus, yield displacement, yield stress, and yield strain [3]. Mineral-to-matrix ratio and carbonate-to-matrix ratios are the strongest predictors of mechanical properties. Less systematic work has been performed on human tissue, but crystallinity, which is also correlated with both mineral-to-matrix ratio and carbonate-to-phosphate, has been related to modulus, yield stress, and fracture stress [81]. As expected, cortical bone mechanical properties vary with anatomic site along a long bone, and crystallinity and other parameters do as well, although the same Raman/material property relation seems to hold at any site.

### Age-related Changes in Bone

Bone Raman spectra change systematically with tissue age in cortical bone from the femurs of female rats ranging in age from 3 to 24 months old [3]. The mineral phosphate band at 960  $\text{cm}^{-1}$  (relative to matrix collagen) and carbonate band at 1070  $\text{cm}^{-1}$  (relative to mineral phosphate) increase with tissue age. Raman spectra of young and aged rat bone (Fig. 2) show this carbonate content variation. Mineral crystallinity is also found to increase with tissue age. These increases accompany the deterioration of the structural and tissue-level mechanical properties of aging

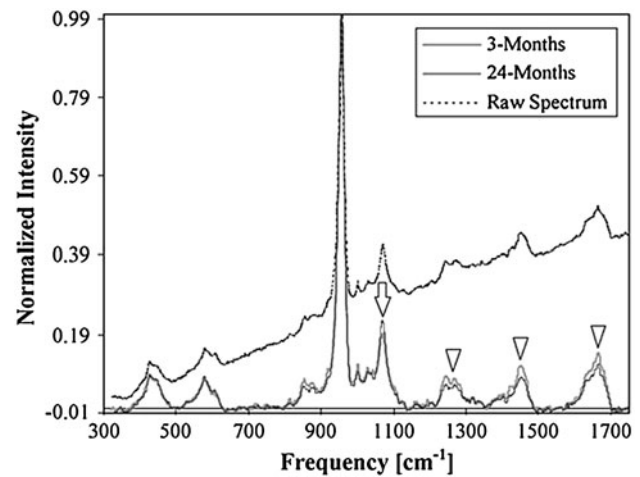


**Fig. 2** Typical spectral profiles taken from young and aged rats. Intensity of each spectrum was normalized by its peak intensity value at the phosphate symmetric stretch band; thus, the normalized intensity at a given band represents the amount of the corresponding species per amount of mineral. The raw spectrum was shifted and normalized to fit within the scales of the baseline-corrected spectra. Collagen-related bands (arrowheads) of young rats had greater intensities than those of old rats, indicating a lower level of mineralization. On the other hand, the intensity of symmetric carbonate stretch band (arrow) was greater for the older rats, indicating a greater level of carbonate substitution in phosphate positions (Adapted from Akkus O, Adar F, Schaffler MB. Age-related changes in physicochemical properties of mineral crystals are related to impaired mechanical function of cortical bone. *Bone*. 2004;34: 443–453 with permission of Elsevier Inc).

cortical bone. Similar age-related trends of increased mineral-to-matrix and carbonate-to-phosphate ratios have been reported for human cortical bone [82], although mineral crystallinity remained unchanged. These published results are for males aged 52 to 85 years. Combined with coefficient of variation measurements, variations about the means of the mineral-to-matrix ratio, carbonate-to-phosphate ratio, and mineral crystallinity became tighter with age. Moreover, histograms of bone mineral properties are non-Gaussian. For example, the mineral distribution for older bone is skewed to the high side of the mean mineralization value. These changes are attributed to decreased heterogeneity of bone mineral properties with age.

### Osteoporosis

Dual-energy X-ray absorptiometry (DXA) T-score is the gold standard for diagnosis of osteopenia and osteoporosis; however, DXA is only a moderate predictor of fracture risk [10, 16, 47, 72]. However, bone Raman spectra contains molecular composition information related to fracture risk. A comparison of specimens from low trauma fracture victims and control subjects matched for age and bone volume fraction [48] showed fractured specimens had a

higher carbonate-to-phosphate ratio than control subjects in the cortical bone but not in cancellous bone. That no differences were found in cancellous bone was attributed to high levels of remodeling and high variability in chemical composition characteristic of this bone. Fracture cases tended to have higher mineral-to-matrix ratios ( $p = 0.11$ ) and higher carbonate-to-amide I ratios ( $p = 0.04$ ). The explanation given was that fractured bone tissue underwent greater remodeling and was undermineralized as a result.

This study indicated Raman spectra contain compositional information predictive of fracture risk. An ongoing 5-year prospective study (R. R. Recker, Creighton University, PI) on 120 postmenopausal women is testing the fracture risk prediction ability of several physicochemical techniques. The Morris laboratory is the Raman spectroscopy test site. Confirmation of the preliminary findings and application of more sophisticated data reduction methods, along with the development of noninvasive Raman spectroscopy, could lead to new Raman-based methods for assessing fracture risk and monitoring therapeutic intervention.

The composition of trabecular bone in rat models of osteoporosis induced by spinal cord injury (SCI) has been studied by Raman spectroscopy [69]. Measurements were made at the distal femur and humerus at 1, 2, 3, and 5 weeks postsurgery. In comparison to age-matched controls, a decrease in mineral (relative to the  $\text{CH}_2$  band at  $1450\text{ cm}^{-1}$ ) by greater than 20% in the femur and approximately 12% in the humerus was found in the SCI group. The decrease in mineral-to-matrix ratios after SCI could be attributed to changes in hormone levels, which have been known to regulate bone remodeling [33]. However, correlative data on hormone levels are lacking and the hormone responsible for the decrease in mineral-to-matrix ratios has yet to be determined.

Anabolic agents such as PTH 1-34 (teriparatide) in osteoporosis therapies are increasing. Raman spectroscopy can be used to monitor effects on bone mineral and matrix quality. Even before the development of noninvasive techniques, Raman spectroscopy was used to follow temporal-dependent effects of PHT on mineralization [59]. Only mineral-to-matrix ratio was reported, and other measures of bone quality such as crystallinity and carbonate-to-phosphate ratio and collagen quality data have not been reported. This work suggests that *in vivo* (and potentially noninvasive) Raman spectroscopy may be useful in animal and possibly in human subjects studies of anabolic agents now under development. In another study, Raman spectroscopy was used to investigate the effects of a combined vitamin K and risedronate therapy in ovariectomized (OVX) mouse models of osteoporosis [46]. Prior treatment of OVX mice with vitamin  $\text{K}_2$  substantially improved the efficiency of risedronate, which in turn

increased femur bone strength compared with OVX controls. Although mineral crystallinity remained unchanged in all the groups, the cortical mineral-to-matrix ratio was lower in OVX mice treated with vitamin  $\text{K}_2$  at 8 weeks. When the vitamin  $\text{K}_2$  treatment was discontinued at Week 8, mineral-to-matrix ratios increased at Week 16. Despite beneficial effects of the 8-week vitamin  $\text{K}_2$  treatment on cortical bone matrix, the increased mineral-to-matrix ratio was attributed to either collagen degradation or decreased collagen synthesis.

### Mouse Models of Bone Properties

Although bone mineral and collagen compositional contributors to bone quality have been studied in greater detail, the role of NCPs to bone material properties remains unclear. Although NCPs in bone are not observed spectroscopically by Raman spectroscopy, their effect on bone composition can be studied by comparing bone tissues from wild-type and knockout animals. For instance, Raman studies show that mineral-to-matrix ratios in osteopontin-deficient (OPN $-/-$ ) mice with ages of 12 weeks or less are lower than in wild type (OPN $+/+$ ) mice [35]. Mechanical studies show young OPN $-/-$  mice have lower hardness and elastic modulus compared with OPN $+/+$  mice, confirming osteopontin's role in the early stages of mineralization. Raman measurements on femoral bones from fibrillin 2 (Fbn2 $-/-$ ) and (OC $-/-$ ) knockout mice have also been conducted and correlated with mechanical measurements [36]. For example, substantial intrabone variation in mechanics and crystallinity were reported, especially in the midcortical section of OC $-/-$  mice when compared with OC $+/+$  controls. The carbonate-to-phosphate ratio decreased in OC $-/-$  mice, which in turn reduced bone tissue hardness more than elasticity. This result suggests that OC plays a role in the growth of apatite crystals in bone by increasing the degree of carbonate substitution.

Raman studies on femora obtained from a murine model of skeletal fragility (SAMP6) showed evidence of reduced collagen content (ie, reduced collagen-to-mineral ratios) and a slight reduction in mineral crystallinity [70]. The reduced bone bending strength observed in SAMP6 mice can be attributed in part to reduced collagen content, whereas light microscopy confirmed the presence of poorly organized collagen fibers.

### Orientation Effects

Polarized white light used in microscopy can be used to study oriented tissues such as collagen [9]. Likewise, polarization can be used with Raman spectroscopy to

provide orientation-related information for the tissue components. This capability has been elegantly demonstrated in a study of human osteonal and interstitial tissue [37, 38]. Because of the circular pattern of mineral deposition around osteons and the regularly progressing orientation of lamellae, polarized light images show rings of alternating high and low mineral and collagen intensity and clearly defined interstitial regions. Combining acoustic impedance measurements with polarized Raman spectroscopy [32] can provide site-matched compositional, structural, and elastic information. These types of studies are important in understanding whether the alternating lamellar structures help protect osteons from catastrophic failure [31]. However, mineral crystallites and collagen fibrils are not ideally oriented. Polarized Raman spectroscopy allows study of the imperfections in orientation [61] to provide insight into tissue failure mechanisms.

### Chemical and Radiologic Insults to Bone Tissue

Abnormal bone composition caused by external agents is easily detected by Raman spectroscopy. One example is formation of undermineralized osteocyte lacunae accompanying glucocorticoid administration to estrogen-deficient mice [42]. Undermineralization correlates well with reduced elastic modulus. This result is also further confirmation that Raman spectroscopic measurements can be usefully correlated with modulus measurements.

Composition changes accompanying osteoradionecrosis of the mandible (induced by radiation therapy for oral cancer) have been interpreted as the result of destruction of vascularity and marrow in the jaw, resulting in loss of lipids and collagen and causing changes in the structure of the bone mineral itself [41]. These composition changes have been detected by Raman spectroscopy in specimens from people who had bone tissue removed as a result of cancer in soft tissue of the jaw. Raman spectroscopy may enable monitoring for osteonecrosis of the jaw that can accompany oral surgery on patients taking bisphosphonates, although further study is needed. The mandible should be accessible using noninvasive fiberoptic Raman spectroscopy as described later in this review.

### Fracture and Other Mechanical Insults to Bone

Raman bands vary in position and intensity with mechanical load on most materials, including bone. Raman spectroscopic imaging shows regions of alternating high and low compression in specimens of bovine cortical bone [60]. Changes in the phosphate  $959\text{ cm}^{-1}$  band position as a function of mechanical load [13, 17, 51] are easily

studied. Changes in mineral bands result from changes in ion spacing with load. In contrast, changes in collagen spectra probably reflect the known distortion of crosslinks.

Spectral properties of collagen and mineral are altered along the edges of microcracks [75] and within indents made in bone tissue [15, 48]. Alterations in collagen spectra occur only near the edges of indents, suggesting shear forces distort and probably rupture crosslinks. Crosslink rupture is an accepted failure mechanism for bone [71]. The loading effect has been further studied [22] by loading bone to close to the point of failure, leaving it in a highly stressed state. The stress field observed experimentally by Raman is similar to that predicted by finite element analysis calculations. At fracture boundaries, irregular patterns of mineral loss (mineral-to-matrix ratio decrease) and collagen quality parameter reduction are observed [48]. In human bone, alterations can be seen 1 to 2 mm away from the fracture boundary [48].

The unique ability of Raman spectroscopy to detect spatial changes in mineral composition lends itself to the study of mineral distributions across tendon-to-bone insertion sites of the rotator cuff [79]. Injuries to the rotator cuff tendons of the shoulder are particularly problematic, because they heal poorly even after surgical intervention. In this preliminary study, the insertion sites of five rats were monitored using the relative intensity of the phosphate band at  $960\text{ cm}^{-1}$  to either the  $2490\text{ cm}^{-1}$  or  $1003\text{ cm}^{-1}$  collagen band [79]. The mineral-to-matrix ratios across the insertion site increased linearly ( $R^2 = 0.8$  for five specimens) over a distance of  $120\text{ }\mu\text{m}$  from tendon to bone rather than abruptly as previously inferred from histologic observations [8]. Moreover, narrowing of the  $960\text{ cm}^{-1}$  peak bandwidth indicated that the crystalline ordering within the apatite increases concomitantly with the degree of mineralization [79]. This finding of mineral gradation may explain why uninjured tendon-to-bone connection of the rotator cuff can sustain very high loads. This is supported by a recent combined biomechanical modeling and collagen fiber alignment study [26] in which gradation likely serves to distribute stress more effectively across the transition from a flexible to a rigid material (ie, a tendon-to-bone transition).

Raman spectroscopy has been used to assess the compositional changes associated with healing stress fractures in forelimbs of male adult rats [76]. By applying cyclic compression to the forelimb, stress fractures of increasing severities (30%, 45%, 65%, and 85%) were created. It was reported that whole bone strength fully recovered 14 days after injury together with an apparent 80% increase in bone mineral density. The increase in woven bone was also seen as an approximate 30% increase in the mineral-to-matrix ratio (approximately  $960/2940\text{ cm}^{-1}$  and  $960/1003\text{ cm}^{-1}$ ) observed by Raman spectroscopy. Notable differences

between woven bone and control spectra were observed such as the greater intersite heterogeneity within the same bone, increased bandwidths of the mineral bands, and a downward shift of  $3\text{ cm}^{-1}$  in the position of the  $2940\text{ cm}^{-1}$  collagen matrix band. However, no differences in carbonate substitutions were reported.

### Noninvasive Measurements

An emerging strength of Raman spectroscopy is its ability to measure compositional parameters of bone quality noninvasively using specially designed fiberoptic probes placed on the skin of a subject. The technique is called spatially offset Raman spectroscopy (SORS) [44, 65]. In SORS, conventional Raman spectroscopic instruments are used with specially designed optical probes to enhance subsurface measurements through light-scattering media. Importantly, the instruments are compact enough to sit on a table or desk. Low-resolution composition mapping and tomography are possible. Tissue scatters light in all directions, making it difficult to efficiently collect Raman scatter generated more than 2 to 3 cm below the surface of the skin. Raman spectroscopy of bone at superficial clinically important sites such as the distal radius may prove more practical than measurement at profound sites such as the femoral neck. The first *in vivo* validation studies were performed on anesthetized mice and show good agreement between transcutaneous measurements and exposed bone measurements [65]. *Ex vivo* Raman tomography of the middiaphysis of a canine tibia of a width a thickness of over 30 mm has also been demonstrated [64].

Measurement times for the first-generation prototype systems range from 2 to 3 minutes for a single-point spectrum to as much as 1 hour for tomography. Even with these early implementations, applications to anesthetized animals are expanding. It is likely that this technology can be used to reduce the number of laboratory animals that must be euthanized in longitudinal studies of new devices or pharmaceuticals. This should be particularly beneficial in reducing interanimal variation and in reducing study costs associated with managing large animals such as dogs, sheep, or monkeys. It is still too early to estimate how much development will be needed before clinically important measurements such as prediction of fracture risk of osteoporotic bone can be made on human subjects in clinically acceptable timeframes.

### Discussion

This review surveys the basic properties of bone Raman spectra and the relations of observable bands to

composition-related contributors to bone quality. The goal is to alert the reader to a lively field of physical science whose methodology can address important issues in orthopaedics. Applications to a range of problems in basic bone biology, biomechanics, and bone disorders are summarized. New experimental methods that allow non-invasive measurements of bone quality are introduced, although further development is needed before they are ready for clinical use.

We show Raman spectroscopy provides essentially the same composition-related information that is available in FTIR spectra and emphasize the strengths of Raman spectroscopy as a bone quality measurement tool, especially its applicability to fresh tissue, live animals, and even human subjects and its micron-level spatial resolution. We point out that Raman spectra are generally noisier than infrared spectra and acquisition times are usually longer as a consequence of low efficiency of Raman scattering and the limitations of the existing measurement technologies. The prospective user should be aware of the tradeoffs before choosing one spectroscopy or the other.

We have summarized the current status of Raman correlations with bone properties. Proper validation of these correlations is only now underway, and there is still some disagreement about how to measure at least one important metric: mineral-to-matrix ratio. An informal consensus is forming around use of proline and hydroxyproline bands in the  $830$  to  $880\text{ cm}^{-1}$  spectral range as measures of matrix content, but further validation is needed. At the basic science level, full validation of all of the proposed correlations is the greatest unmet need in bone Raman spectroscopy.

We have summarized a few practical applications that have been addressed by Raman spectroscopy. For the clinician, the evidence pointing to the possibility that fracture risk information may be inherent in bone Raman spectra and the demonstration that Raman spectroscopy can identify necrotic bone tissue may be especially interesting. These findings suggest important diagnostic roles for bone Raman spectroscopy may emerge.

The recent demonstration of noninvasive bone Raman spectroscopy and tomography is especially exciting. The prospect of an information-rich methodology that uses compact and relatively inexpensive instruments, which does not use ionizing radiation, bears close watching. There are still only a few laboratories working in this field and questions of penetration depth and measurement time are still unresolved. Already, Raman spectroscopy and tomography have reached depths 2 to 3 cm below the skin. At these penetration depths, Raman measurements at clinically important sites, including the distal radius, are possible. With further validation and engineering development, an important new clinical tool may emerge.

Finally, what emerges from this review is that bone Raman spectroscopy has proven its worth in the basic science laboratories and is only now entering the translational phase. Basic scientists still need to put more emphasis on validation studies. Engineers are needed to design instruments that can be operated by technicians and that generate outputs in the language of orthopaedics.

**Acknowledgments** We thank Kathryn A. Dooley for her contribution of a bone Raman spectrum to this article. We acknowledge Dr Francis W. L. Esmonde-White for discussions and proofreading of this article.

## References

- Ager JW, Nalla RK, Balooch G, Kim G, Pugach M, Habelitz S, Marshall GW, Kinney JH, Ritchie RO. On the increasing fragility of human teeth with age: a deep-UV resonance Raman study. *J Bone Miner Res.* 2006;21:1879–1887.
- Ager JW, Nalla RK, Breeden KL, Ritchie RO. Deep-ultraviolet Raman spectroscopy study of the effect of aging on human cortical bone. *J Biomed Opt.* 2005;10:034012.
- Akkus O, Adar F, Schaffler MB. Age-related changes in physicochemical properties of mineral crystals are related to impaired mechanical function of cortical bone. *Bone.* 2004;34:443–453.
- Aparicio S, Doty SB, Camacho NP, Paschalis EP, Spevak L, Mendelsohn R, Boskey AL. Optimal methods for processing mineralized tissues for Fourier transform infrared microspectroscopy. *Calcif Tissue Int.* 2002;70:422–429.
- Awonusi A, Morris MD, Tecklenburg MM. Carbonate assignment and calibration in the Raman spectrum of apatite. *Calcif Tissue Int.* 2007;81:46–52.
- Barth HD, Launey ME, MacDowell AA, Ager JW, Ritchie RO. On the effect of X-ray irradiation on the deformation and fracture behavior of human cortical bone. *Bone.* 2010;46:1475–1485.
- Bazin D, Chappard C, Combes C, Carpentier X, Rouziere S, Andre G, Matzen G, Allix M, Thiaudiere D, Reguer S, Jungers P, Daudon M. Diffraction techniques and vibrational spectroscopy opportunities to characterise bones. *Osteoporosis Int.* 2009;20:1065–1075.
- Benjamin M, Kumai T, Milz S, Boszczyk BM, Boszczyk AA, Ralphs JR. The skeletal attachment of tendons—tendon ‘entheses.’ *Comp Biochem Physiol A Mol Integr Physiol.* 2002;133:931–945.
- Beraudi A, Stea S, Bordini B, Baleani M, Viceconti M. Osteon classification in human fibular shaft by circularly polarized light. *Cells Tissues Organs.* 2010;191:260–268.
- Blake GM, Fogelman I. How important are BMD accuracy errors for the clinical interpretation of DXA scans? *J Bone Miner Res.* 2008;23:457–462.
- Boskey A. Bone mineral crystal size. *Osteoporosis Int.* 2003;14(Suppl 5):S16–S20.
- Boskey A, Mendelsohn R. Infrared analysis of bone in health and disease. *J Biomed Opt.* 2005;10:031102.
- Callender AF, Finney WF, Morris MD, Sahar ND, Kohn DH, Kozloff KM, Goldstein SA. Dynamic mechanical testing system for Raman microscopy of bone tissue specimens. *Vibrational Spectroscopy.* 2005;38:101–105.
- Carden A, Morris MD. Application of vibrational spectroscopy to the study of mineralized tissues (review). *J Biomed Opt.* 2000;5:259–268.
- Carden A, Rajachar RM, Morris MD, Kohn DH. Ultrastructural changes accompanying the mechanical deformation of bone tissue: a Raman imaging study. *Calcif Tissue Int.* 2003;72:166–175.
- Cummings SR, Bates D, Black DM. Clinical use of bone densitometry: scientific review. *JAMA.* 2002;288:1889–1897.
- de Carmejane O, Morris MD, Davis MK, Stixrude L, Tecklenburg M, Rajachar RM, Kohn DH. Bone chemical structure response to mechanical stress studied by high pressure Raman spectroscopy. *Calcif Tissue Int.* 2005;76:207–213.
- de Mul FFM, Otto C, Greve J, Arends J, ten Bosch JJ. Calculation of the Raman line broadening on carbonation in synthetic hydroxyapatite. *J Raman Spectrosc.* 1988;19:13–21.
- Dendramis AL, Poser JW, Schwinn EW. Laser Raman spectroscopy of calf bone Gla protein. *Biochim Biophys Acta.* 1983;742:525–529.
- Denson SC, Pommier CJS, Denton MB. The impact of array detectors on Raman spectroscopy. *J Chem Educ.* 2007;84:67.
- Donnelly E, Boskey AL, Baker SP, van der Meulen MC. Effects of tissue age on bone tissue material composition and nanomechanical properties in the rat cortex. *J Biomed Mater Res A.* 2010;92:1048–1056.
- Dooley KA, McCormack J, Fyhrie DP, Morris MD. Stress mapping of undamaged, strained, and failed regions of bone using Raman spectroscopy. *J Biomed Opt.* 2009;14:044018.
- Faibish D, Ott SM, Boskey AL. Mineral changes in osteoporosis: a review. *Clin Orthop Relat Res.* 2006;443:28–38.
- Freeman JJ, Wopenka B, Silva MJ, Pasteris JD. Raman spectroscopic detection of changes in bioapatite in mouse femora as a function of age and in vitro fluoride treatment. *Calcif Tissue Int.* 2001;68:156–162.
- Gamsjaeger S, Roschger P, Klaushofer K, Paschalis EP, Fratzl P. Cortical bone orientation and composition in a mouse model as a function of tissue age vs animal age. *Bone.* 2009;44(Suppl 2):S269–S270.
- Genin GM, Kent A, Birman V, Wopenka B, Pasteris JD, Marquez PJ, Thomopoulos S. Functional grading of mineral and collagen in the attachment of tendon to bone. *Biophys J.* 2009;97:976–985.
- Golcuk K, Mandair GS, Callender AF, Sahar N, Kohn DH, Morris MD. Is photobleaching necessary for Raman imaging of bone tissue using a green laser? *Biochim Biophys Acta.* 2006;1758:868–873.
- Goodyear SR, Gibson IR, Skakle JM, Wells RP, Aspden RM. A comparison of cortical and trabecular bone from C57 black 6 mice using Raman spectroscopy. *Bone.* 2009;44:899–907.
- Gourion-Arsiquaud S, Allen MR, Burr DB, Vashishth D, Tang SY, Boskey AL. Bisphosphonate treatment modifies canine bone mineral and matrix properties and their heterogeneity. *Bone.* 2010;46:666–672.
- Gourion-Arsiquaud S, Burket JC, Havill LM, DiCarlo E, Doty SB, Mendelsohn R, van der Meulen MC, Boskey AL. Spatial variation in osteonal bone properties relative to tissue and animal age. *J Bone Miner Res.* 2009;24:1271–1281.
- Gupta HS, Stachewicz U, Wagermaier W, Roschger P, Wagner HD, Fratzl P. Mechanical modulation at the lamellar level in osteonal bone. *J Mater Res.* 2006;21:1913–1921.
- Hofmann T, Heyroth F, Meinhard H, Franzel W, Raum K. Assessment of composition and anisotropic elastic properties of secondary osteon lamellae. *J Biomech.* 2006;39:2282–2294.
- Jiang SD, Jiang LS, Dai LY. Mechanisms of osteoporosis in spinal cord injury. *Clin Endocrinol (Oxf).* 2006;65:555–565.
- Judex S, Boyd S, Qin Y-X, Miller L, Müller R, Rubin C. Combining high-resolution micro-computed tomography with material composition to define the quality of bone tissue. *Curr Osteoporosis Rep.* 2003;1:11–19.



35. Kavukcuoglu NB, Denhardt DT, Guzelsu N, Mann AB. Osteopontin deficiency and aging on nanomechanics of mouse bone. *J Biomed Mater Res A*. 2007;83:136–144.
36. Kavukcuoglu NB, Patterson-Buckendahl P, Mann AB. Effect of osteocalcin deficiency on the nanomechanics and chemistry of mouse bones. *J Mech Behav Biomed Mater*. 2009;2:348–354.
37. Kazanci M, Roschger P, Paschalis EP, Klaushofer K, Fratzl P. Bone osteonal tissues by Raman spectral mapping: orientation-composition. *J Struct Biol*. 2006;156:489–496.
38. Kazanci M, Wagner HD, Manjubala NI, Gupta HS, Paschalis E, Roschger P, Fratzl P. Raman imaging of two orthogonal planes within cortical bone. *Bone*. 2007;41:456–461.
39. Kohn DH, Sahar ND, Wallace JM, Golcuk K, Morris MD. Exercise alters mineral and matrix composition in the absence of adding new bone. *Cells Tissues Organs*. 2009;189:33–37.
40. Krafft C, Codrich D, Pelizzo G, Sergio V. Raman and FTIR microscopic imaging of colon tissue: a comparative study. *J Biophotonics*. 2008;1:154–169.
41. Lakshmi RJ, Alexander M, Kurien J, Mahato KK, Kartha VB. Osteoradionecrosis (ORN) of the mandible: a laser Raman spectroscopic study. *Appl Spectrosc*. 2003;57:1100–1116.
42. Lane NE, Yao W, Balooch M, Nalla RK, Balooch G, Habelitz S, Kinney JH, Bonewald LF. Glucocorticoid-treated mice have localized changes in trabecular bone material properties and osteocyte lacunar size that are not observed in placebo-treated or estrogen-deficient mice. *J Bone Miner Res*. 2006;21:466–476.
43. Legros R, Balmain N, Bonel G. Age-related changes in mineral of rat and bovine cortical bone. *Calcif Tissue Int*. 1987;41:137–144.
44. Matousek P, Draper ER, Goodship AE, Clark IP, Ronayne KL, Parker AW. Noninvasive Raman spectroscopy of human tissue in vivo. *Appl Spectrosc*. 2006;60:758–763.
45. Matousek P, Stone N. Emerging concepts in deep Raman spectroscopy of biological tissue. *Analyst*. 2009;134:1058–1066.
46. Matsumoto Y, Mikuni-Takagaki Y, Kozai Y, Miyagawa K, Naruse K, Wakao H, Kawamata R, Kashima I, Sakurai T. Prior treatment with vitamin K(2) significantly improves the efficacy of risedronate. *Osteoporos Int*. 2009;20:1863–1872.
47. McCreddie BR, Goldstein SA. Biomechanics of fracture: is bone mineral density sufficient to assess risk? *J Bone Miner Res*. 2000;15:2305–2308.
48. McCreddie BR, Morris MD, Chen TC, Sudhaker Rao D, Finney WF, Widjaja E, Goldstein SA. Bone tissue compositional differences in women with and without osteoporotic fracture. *Bone*. 2006;39:1190–1195.
49. Mendelsohn R, Paschalis EP, Boskey AL. Infrared spectroscopy, microscopy, and microscopic imaging of mineralizing tissues: spectra-structure correlations from human iliac crest biopsies. *J Biomed Opt*. 1999;4:14–21.
50. Morris MD, Crane NJ, Gomez LE, Ignelzi MA. Compatibility of staining protocols for bone tissue with Raman imaging. *Calcif Tissue Int*. 2004;74:86–94.
51. Morris MD, Finney WF, Rajachar RM, Kohn DH. Bone tissue ultrastructural response to elastic deformation probed by Raman spectroscopy. *Faraday Discuss*. 2004;126:159–168; discussion 169–183.
52. Parkesh R, Mohsin S, Lee TC, Gunnlaugsson TC. Histological, spectroscopic, and surface analysis of microdamage in bone: toward real-time analysis using fluorescent sensors. *Chem Mater*. 2007;19:1656–1663.
53. Paschalis EP, DiCarlo E, Betts F, Sherman P, Mendelsohn R, Boskey AL. FTIR microspectroscopic analysis of human osteonal bone. *Calcif Tissue Int*. 1996;59:480–487.
54. Paschalis EP, Shane E, Lyritis G, Skarantavos G, Mendelsohn R, Boskey AL. Bone fragility and collagen cross-links. *J Bone Miner Res*. 2004;19:2000–2004.
55. Paschalis EP, Verdelsis K, Doty SB, Boskey AL, Mendelsohn R, Yamauchi M. Spectroscopic characterization of collagen cross-links in bone. *J Bone Miner Res*. 2001;16:1821–1828.
56. Pasteris JD, Wopenka B, Freeman JJ, Rogers K, Valsami-Jones E, van der Houwen JAM, Silva MJ. Lack of OH in nanocrystalline apatite as a function of degree of atomic order: implications for bone and biomaterials. *Biomaterials*. 2004;25:229–238.
57. Penel G, Delfosse C, Descamps M, Leroy G. Composition of bone and apatitic biomaterials as revealed by intravital Raman microspectroscopy. *Bone*. 2005;36:893–901.
58. Penel G, Leroy G, Rey C, Bres E. MicroRaman spectral study of the PO<sub>4</sub> and CO<sub>3</sub> vibrational modes in synthetic and biological apatites. *Calcif Tissue Int*. 1998;63:475–481.
59. Pettway GJ, Schneider A, Koh AJ, Widjaja E, Morris MD, Meganck JA, Goldstein SA, McCauley LK. Anabolic actions of PTH (1-34): use of a novel tissue engineering model to investigate temporal effects on bone. *Bone*. 2005;36:959–970.
60. Pezzotti G. Raman piezo-spectroscopic analysis of natural and synthetic biomaterials. *Anal Bioanal Chem*. 2005;381:577–590.
61. Raghavan M, Sahar N, Wilson RH, Mycek M-A, Pleshko N, Kohn DH, Morris MD. Quantitative polarized Raman spectroscopy in highly turbid bone tissue. *J Biomed Opt*. 2010;15:037001.
62. Rohleder D, Kocherscheidt G, Gerber K, Kiefer W, Kohler W, Mocks J, Petrich W. Comparison of mid-infrared and Raman spectroscopy in the quantitative analysis of serum. *J Biomed Opt*. 2005;10:031108.
63. Schlucker S, Schaeberle MD, Huffman SW, Levin IW. Raman microspectroscopy: a comparison of point, line, and wide-field imaging methodologies. *Anal Chem*. 2003;75:4312–4318.
64. Schulmerich MV, Cole JH, Dooley KA, Morris MD, Kreider JM, Goldstein SA, Srinivasan S, Pogue BW. Noninvasive Raman tomographic imaging of canine bone tissue. *J Biomed Opt*. 2008;13:020506.
65. Schulmerich MV, Cole JH, Kreider JM, Esmonde-White F, Dooley KA, Goldstein SA, Morris MD. Transcutaneous Raman spectroscopy of murine bone in vivo. *Appl Spectrosc*. 2009;63:286–295.
66. Schulmerich MV, Dooley KA, Morris MD, Vanasse TM, Goldstein SA. Transcutaneous fiber optic Raman spectroscopy of bone using annular illumination and a circular array of collection fibers. *J Biomed Opt*. 2006;11:060502.
67. Schulmerich MV, Dooley KA, Vanasse TM, Goldstein SA, Morris MD. Subsurface and transcutaneous Raman spectroscopy and mapping using concentric illumination rings and collection with a circular fiber-optic array. *Appl Spectrosc*. 2007;61:671–678.
68. Shea DA, Morris MD. Bone tissue fluorescence reduction for visible laser Raman spectroscopy. *Applied Spectroscopist*. 2002;56:182–186.
69. Shen J, Fan L, Yang J, Shen AG, Hu JM. A longitudinal Raman microspectroscopic study of osteoporosis induced by spinal cord injury. *Osteoporos Int*. 2010;21:81–87.
70. Silva MJ, Brodt MD, Wopenka B, Thomopoulos S, Williams D, Wassen MH, Ko M, Kusano N, Bank RA. Decreased collagen organization and content are associated with reduced strength of demineralized and intact bone in the SAMP6 mouse. *J Bone Miner Res*. 2006;21:78–88.
71. Silver FH, Kato YP, Ohno M, Wasserman AJ. Analysis of mammalian connective tissue: relationship between hierarchical structures and mechanical properties. *J Long Term Eff Med Implants*. 1992;2:165–198.
72. Stone KL, Seeley DG, Lui LY, Cauley JA, Ensrud K, Browner W, Nevitt MC, Cummings SR, Osteoporotic Fractures Research Group. BMD at multiple sites and risk of fracture of multiple types: long-term results from the Study of Osteoporotic Fractures. *J Bone Miner Res*. 2003;18:1947–1954.

73. Tarnowski CP, Ignelzi MA, Morris MD. Mineralization of developing mouse calvaria as revealed by Raman microspectroscopy. *J Bone Miner Res.* 2002;17:1118–1126.
74. Tarnowski CP, Ignelzi MA, Wang W, Taboas JM, Goldstein SA, Morris MD. Earliest mineral and matrix changes in force-induced musculoskeletal disease as revealed by Raman microspectroscopic imaging. *J Bone Miner Res.* 2004;19:64–71.
75. Timlin JA, Carden A, Morris MD, Rajachar RM, Kohn DH. Raman spectroscopic imaging markers for fatigue-related microdamage in bovine bone. *Anal Chem.* 2000;72:2229–2236.
76. Uthgenannt BA, Kramer MH, Hwu JA, Wopenka B, Silva MJ. Skeletal self-repair: stress fracture healing by rapid formation and densification of woven bone. *J Bone Miner Res.* 2007;22:1548–1556.
77. Wallace JM, Golcuk K, Morris MD, Kohn DH. Inbred strain-specific effects of exercise in wild type and biglycan deficient mice. *Ann Biomed Eng.* 2010;38:1607–1617.
78. Wallace JM, Golcuk K, Morris MD, Kohn DH. Inbred strain-specific response to biglycan deficiency in the cortical bone of C57BL/6/129 and C3H/He mice. *J Bone Miner Res.* 2009;24:1002–1012.
79. Wopenka B, Kent A, Pasteris JD, Yoon Y, Thomopoulos S. The tendon-to-bone transition of the rotator cuff: a preliminary Raman spectroscopic study documenting the gradual mineralization across the insertion in rat tissue samples. *Appl Spectrosc.* 2008;62:1285–1294.
80. Yeni YN, Yerramshetty J, Akkus O, Pechey C, Les CM. Effect of fixation and embedding on Raman spectroscopic analysis of bone tissue. *Calcif Tissue Int.* 2006;78:363–371.
81. Yerramshetty JS, Akkus O. The associations between mineral crystallinity and the mechanical properties of human cortical bone. *Bone.* 2008;42:476–482.
82. Yerramshetty JS, Lind C, Akkus O. The compositional and physicochemical homogeneity of male femoral cortex increases after the sixth decade. *Bone.* 2006;39:1236–1243.